

Cyber-physical systems approach to optimization in wind engineering: parapet wall design

Michael L. Whiteman ^a, Brian M. Phillips ^b, Pedro L. Fernández Cabán ^c, Forrest J. Masters ^d, Jennifer A. Rice ^e, Justin R. Davis ^f

^a University of Maryland, College Park, Maryland, USA, mlwii@umd.edu
^b University of Maryland, College Park, Maryland, USA, bphilli@umd.edu
^c University of Florida, Gainesville, Florida, USA, plfernandez@ufl.edu
^d University of Florida, Gainesville, Florida, USA, masters@eng.ufl.edu
^e University of Florida, Gainesville, Florida, USA, justin.r.davis@essie.ufl.edu

ABSTRACT: This paper explores the use of cyber-physical systems (CPS) for optimal design in wind engineering. The approach combines the accuracy of physical wind tunnel testing with the ability to efficiently explore a solution space using numerical optimization algorithms. The approach is fully automated, with experiments executed in a boundary layer wind tunnel (BLWT), sensor feedback monitored by a high-performance computer, and actuators used to bring about physical changes in the BLWT. Because the model is undergoing physical change as it approaches the optimal solution, this approach is given the name "loop-in-the-model" testing.

The building selected for this study is a low-rise structure with a parapet wall of variable height. Parapet walls alter the location of the roof corner vortices, alleviating large suction loads on the windward facing roof corner and edges and setting up an interesting optimal design problem. In the BLWT, the model parapet height is adjusted using servo-motors to achieve a particular design. The model surface is instrumented with pressure taps to measure the envelope pressure loading. The taps are densely spaced on the roof to provide sufficient resolution to capture the change in roof corner vortex formation. Experiments are conducted using a boundary BLWT located at the University of Florida Natural Hazard Engineering Research Infrastructure (NHERI) Experimental Facility.

The proposed CPS approach enables the optimal solution to be found quicker than brute force methods, in particular for complex structures with many design variables. The parapet wall provides a proof-of-concept study with a single design variable that has a non-monotonic influence on a structure's wind load. This study focuses on envelope load effects, seeking the parapet height that minimizes roof and parapet wall suction loading. Implications are significant for more complex structures where the optimal solution may not be obvious and cannot be reasonably determined with traditional experimental or computational methods.

KEYWORDS: Cyber-physical systems, optimization, boundary-layer wind tunnel, parapet wall, NHERI

1 INTRODUCTION

Boundary layer wind tunnels (BLWT) remain a leading tool in wind engineering to characterize the pressure loading on wind-sensitive structures. In particular, BLWT testing is valuable when studying new structures for which the simplified provisions of ASCE 7-10 are inadequate or computational fluid dynamics approaches cannot be applied with confidence [1]. While BLWT

testing has remained an industry standard for decades, there have been many recent advances in computationally-based optimization techniques for structural design. Meta-heuristic algorithms such as particle swarm and genetic algorithms are problem-independent algorithms that efficiently explore a complex solution space, providing new opportunities to study multi-variate and multi-objective optimization problems. While new optimization techniques have promise for delivering cost-effective design solutions for wind-sensitive structures, they must be combined with a method such as BLWT testing to evaluate the candidate solutions.

This study proposes the use of cyber-physical systems (CPS) for optimal design in wind engineering. The study will create a proof-of-concept that demonstrates the potential for replacing laborious trial-and-error design approaches with cyberinfrastructure-augmented BLWT modeling that produces optimal designs faster than purely experimental methods and with a higher degree of realism than purely computational methods. The approach is fully automated, with experiments executed in a BLWT, sensor feedback monitored by a high-performance computer, and optimization techniques used to bring about physical changes to the structural model in the BLWT. Because the model is undergoing physical change as it approaches the optimal solution, this approach is given the name "loop-in-the-model" testing. The CPS framework is illustrated in Figure 1.

The building selected for this study is a low-rise structure with a parapet wall of variable height. The sharp edges on bluff bodies, in particular windward roof edges on low-rise structures, cause a separation of the boundary layer and generate vortex flow with large suction loading. These loads are particularly severe for oblique approaching wind angles. Parapets are common on industrial and commercial buildings and help to alleviate extreme roof wind suction loads [2-5]. Parapet walls alter the location of the roof corner vortex and mitigate extreme corner and edge suction loads on the roof of the building. Conversely, parapet walls increase the downward roof loads which combine with other roof loads. ASCE 7-10 contains basic design guidance with regard to parapet loading, however it is not refined enough to infer what constitutes an optimal height or configuration.

In this study, the model parapet height is adjusted automatically using servo-motors to reach a particular candidate design. The building envelope is instrumented with pressure taps to measure the envelope pressure loading. The taps are densely spaced on the roof to provide sufficient resolution to capture the change in roof corner vortex formation. Experiments are conducted using a BLWT located at the University of Florida Natural Hazard Engineering Research Infrastructure (NHERI) Experimental Facility.

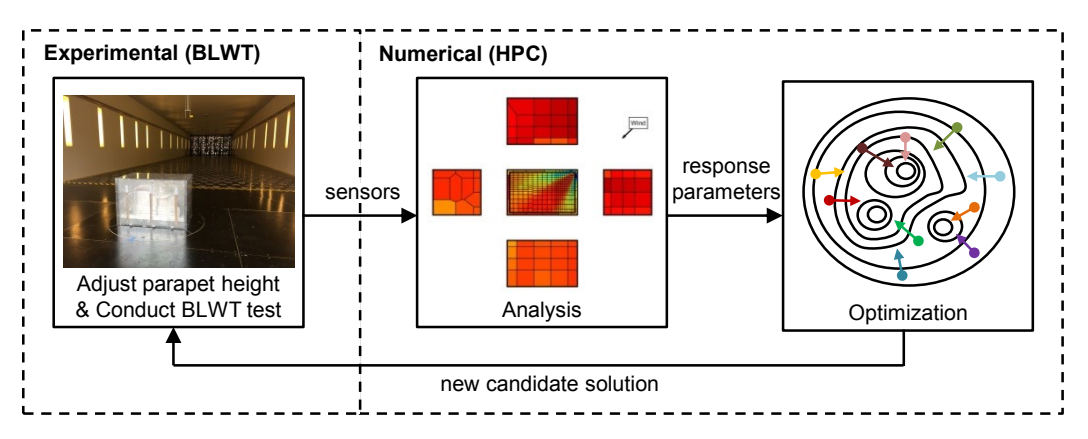


Figure 1. Diagram of CPS framework for optimal design under wind hazards



2 PARTICLE SWARM OPTIMIZATION

Particle swarm optimization (PSO) is a population-based stochastic optimization technique. PSO mimics social behavior where a population of individuals adapts to its environments by discovering and jointly exploring promising regions. This swarm intelligence method is based on the simulation of social interactions of members of a species, such as the movement of flocks of birds, schools of fish, and swarm of bees. Particle swarm optimization was inspired by evolutionary programming, genetic algorithms, and evolution strategies and shares similarities with genetic algorithms and evolutionary algorithms.

Particle swarm optimization is a non-gradient-based, meta-heuristic optimization method [6]. Non-gradient-based optimization techniques are especially useful in solving problems in structural engineering due to their versatility in handling multiple design variables. Particle swarm optimization efficiently explores a large number of candidate solutions over a large search space without prematurely converging, which can lead to non-intuitive solutions. The basic technique is easy to program because it is an inherently iterative process reliant on only a few formulas to govern the iterations. Also, the problem definition does not require continuity and is capable of handling nonlinear, nonconvex design spaces. Complexities can arise in the analysis of candidate solutions, the calculation of the objective function, application of constraints, and ensuring sufficient balance between exploration and exploitation of the design space. As a meta-heuristic method, there is no guarantee that a global optimal solution, or even bounded solution will be found [7]. Because the solution is not necessarily optimal, the solution from a PSO algorithm is more precisely termed a sub-optimal solution. The technique is relatively new with limited studies in structural engineering; however research is actively being conducted to improve this optimization approach with specific structural engineering considerations.

3 EFFECTS OF WIND ON LOW-RISE BUILDINGS WITH PARAPETS

Building detailing has a large influence on the distribution of pressures over the roof surface in both magnitude and direction. With regard to structures with parapet walls, most research focuses on local pressure distributions on the roof surface, as in components and cladding. Studies also include the use of parapets with non-uniform or modified geometries to reduce the extreme suction loads caused by the corner vortices [2]. Additionally, a few studies consider the effect of parapets on the underlying structural members [3, 9]. Recent studies have uncovered inconsistencies with previous research. These inconsistencies are likely the result of an insufficiently dense region of pressure taps in the upwind corner of the roof of the model, leading to the true peak suction pressure values not being measured [2, 3, 10]. Thus, it is essential to have a very high density of pressure taps in the upwind corner region to ensure that the peak suction pressures are captured.

Wind approaching at oblique angles to a building with a flat roof produces strong vortices near the upwind corner and edges of the roof [10]. These vortices are similar to the vortices that are produced at the leading edge of delta type wings and, as such, are also known as delta wing vortices. These vortices create an area of high suction on the surface of the roof near the corner [11]. Solid, continuous perimetric parapets taller than 1 m act to reduce both the mean and peak pressure coefficients in the corner region of these buildings. Most building codes, such as ASCE 7-10, allow for a pressure reduction over different regions of a roof in the presence of parapets; however there has not been extensive research conducted regarding accurate regions of reduction

based upon the geometry of the building and parapet or on the optimal height of a parapet for a given low-rise building [1]. Additionally, research has primarily focused on the corner zones of roofs with limited research focusing on the edge and interior zones. The research regarding the edge and interior zones has mainly focused on mitigating local loading through the use of alternative geometries and not much regarding the effect of different heights of solid, perimetric parapets or on the optimal height of solid, perimetric parapets [5].

4 MODEL DEVELOPMENT

4.1 Design variable

Candidate design solutions must be physically created in the BLWT such that their envelope wind loads are accurately measured. For this proof-of-concept study, a single controllable design variable is sufficient to demonstrate the cyber-physical approach to optimization. Additionally, by limiting the study to a single design variable, unnecessary mechanical complexity is avoided and focus is instead placed on the optimization framework.

The design parameter selected is the parapet wall height of a low-rise building. The outer wall of the model is actuated by four stepper motors, one at each corner of the model. The inner core of the model remains stationary, maintaining a constant building height. As the outer wall rises above the inner model, a parapet wall is created. Strips made from Teflon PTFE are used between the inner model and outer wall to achieve smooth linear actuation. A foam gasket is used between the outer wall and the turntable to allow the outer wall to move while preventing air from leaking around the model. The model is shown in Figure 2, including the inner model (stationary) and outer wall (vertically movable).

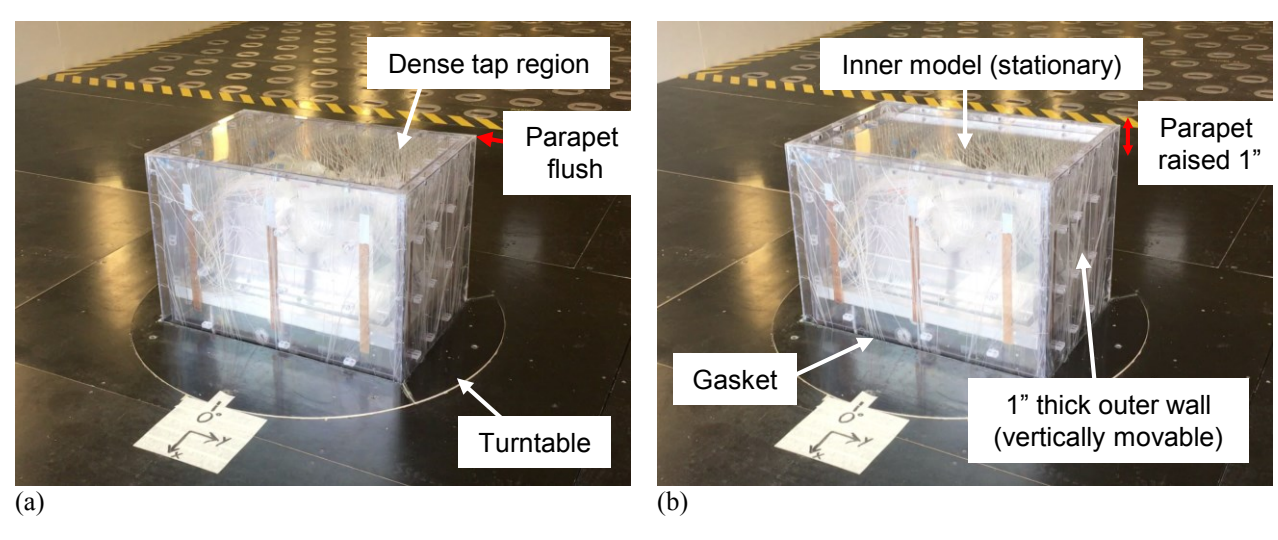


Figure 2. (a) Building model with a 0 inch parapet wall and (b) a 1 inch parapet wall

The linear actuation of the outer wall around the inner core of the model is achieved using of Nanotec stepper motors. These motors are connected to the outer wall using polycarbonate triangular supports installed in the bottom corners. A PVC pipe is installed on the outside of the drive shaft of the stepper motor to protect the shaft from coming into contact with any urethane tubing. The stepper motor and its installation are shown in Figure 3. The setup for controlling the stepper motors is given in Figure 4. Data (i.e., commands from the coordinating computer) and



power are passed through a slip ring on the BLWT turntable. A Raspberry Pi 3 within the turntable then sends commands to the stepper motor controllers, which in turn actuate the stepper motors. Encoders on the stepper motors provide feedback to ensure the desired displacement is reached in all four stepper motors.

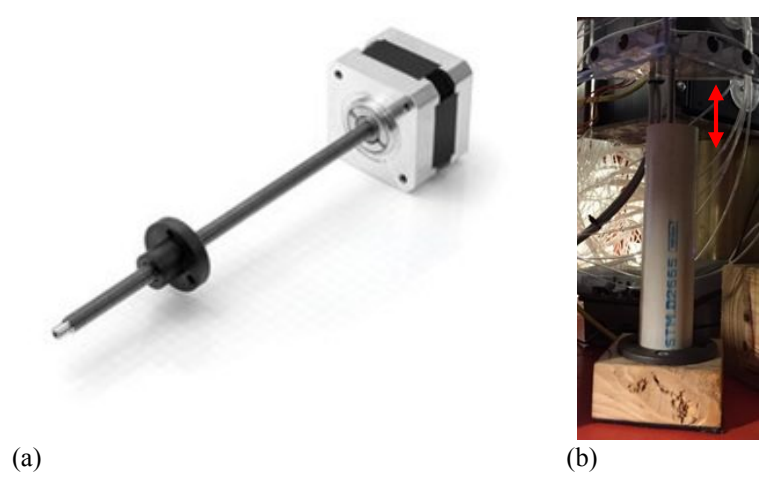


Figure 3. (a) Stepper motor and (b) stepper motor installed in corner of parapet wall with PVC shield

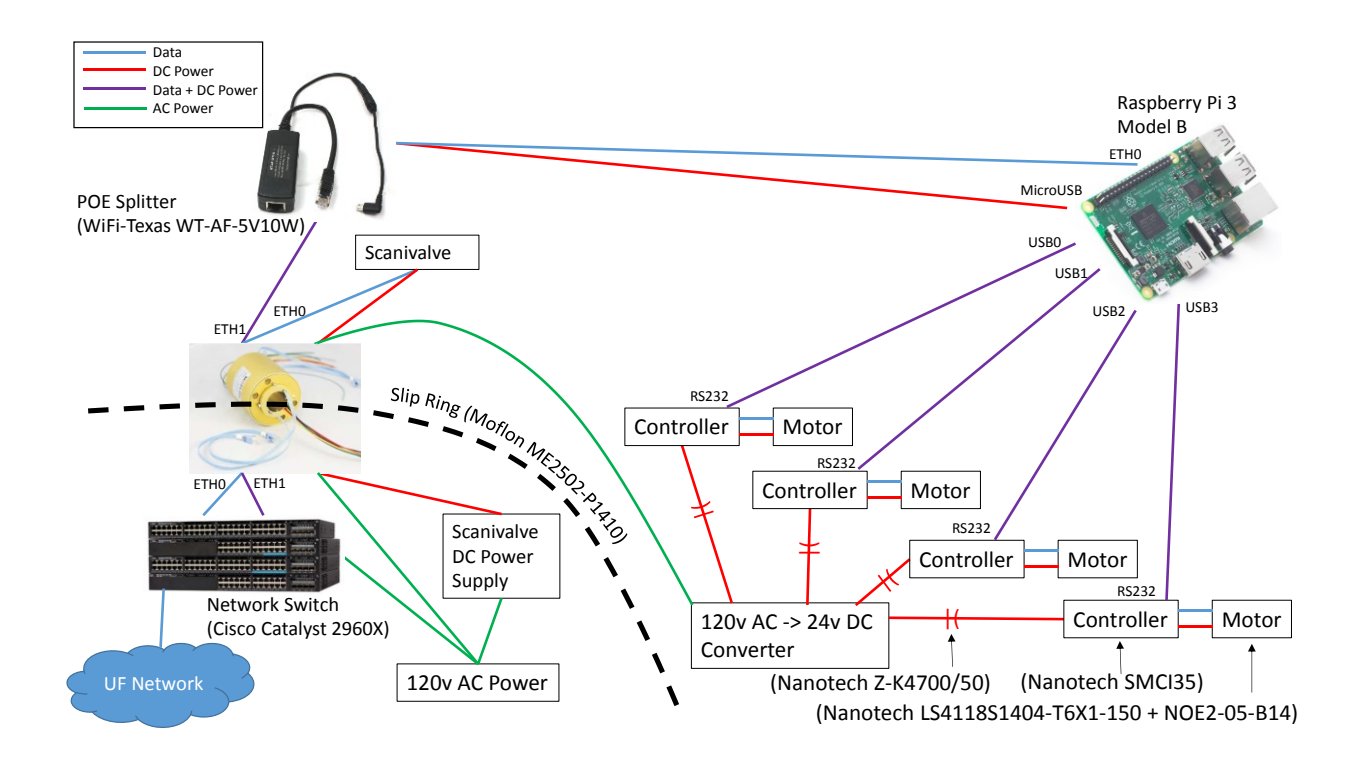


Figure 4. Wiring diagram for stepper motor control

4.2 *Model Geometry*

The low-rise building with a parapet wall is modeled after a two-story office building. The model and outer wall actuation system must fit within the 40 inch diameter turntable. Additionally, a length-to-width ratio of 1.5 is desired to create a rectangular model building. Model dimensions are selected as 29.25 inches × 19.50 inches in plan with a height of 20 inches.

By actuating the outer wall, a parapet wall of up to 5 inches model-scale is created. Urethane tubing and pressure taps are installed on the outer and inner sides of the parapet wall. This requires a total thickness of the model parapet wall (and thus outer wall) of at least 1 inch to accommodate the thickness of polycarbonate sheets, tubulation (metal ends of the urethane tubing), and minimum bend radius of 0.5 inches for the 0.063 inch diameter urethane tubing. The pressure taps on the outer and inner parapet walls are staggered to permit a thinner model parapet wall. The taps and tubing of the inner model and outer wall are shown in Figure 5.

Based on the physical model dimensions and the target two-story office building, a model to full-scale ratio of 1:18 is selected. This corresponds to a building with full-scale dimensions of 29.625 feet × 44.4375 feet in plan, 30 feet tall, and a parapet that is 1.5 feet thick. According to the Building Code Requirements for Masonry Structures, parapet walls should have a thickness of at least 8 inches [12]. The building model represents a realistic two-story full-scale building with a two by three bay steel frame.





Figure 5. (a) Taps and tubing of inner model (stationary) and (b) taps and tubing of outer wall (movable)

5 EXPERIMENTAL SETUP

5.1 Experimental equipment

The pressures on the model building surfaces are measured using Scanivalve ZOC33 pressure scanners. Experiments are conducted using a BLWT located at the University of Florida Natural Hazard Engineering Research Infrastructure (NHERI) Experimental Facility. The BLWT is 6.1 m wide with a 1 m turntable centered along the 6.1 m width 31.75 m downwind of 8 fans. The fans are kept at 1050 RPM for all testing, which corresponds to a reference height velocity of approximately 14 m/s. The the model building installed in the BLWT is shown in Figure 6.





Figure 6. Boundary layer wind tunnel with model low-rise building, upwind view

5.2 Tap tributary areas

The tributary area of a particular tap describes the area over which the tap's pressure is assumed to be acting. In this model, tap locations are variable due to the movable outer wall. Based on the parapet wall height, exposed tap locations and surface areas are first calculated. Then, the tap tributary areas are calculated using Voronoi diagrams derived from Delaney triangulation. This process is both reproducible and automated, which is particularly important because the geometry of the building changes with every candidate solution. The taps and tributary areas for the model with a parapet wall of 5 inches are depicted in the flattened view of Figure 7. The walls of the building are given by Surfaces 1 to 4. As the walls extend above the roof (from actuation), Surfaces 1 to 4 also form the outer parapet walls. The inner parapet walls are given by Surfaces 6 to 9. The edges that join the outer walls (Surfaces 1 to 4) and the inner parapet walls (Surfaces 6 to 9) in Figure 7 are at the same height in the model. I.e., the walls are flattened by rotating about the top of the parapet wall. Surfaces 5 and 10 are the top of the parapet wall and the roof, respectively. As the parapet height increases, the tributary areas for both the outer wall and inner parapet walls increase while the tributary areas for the top of the parapet wall and the roof remain constant.

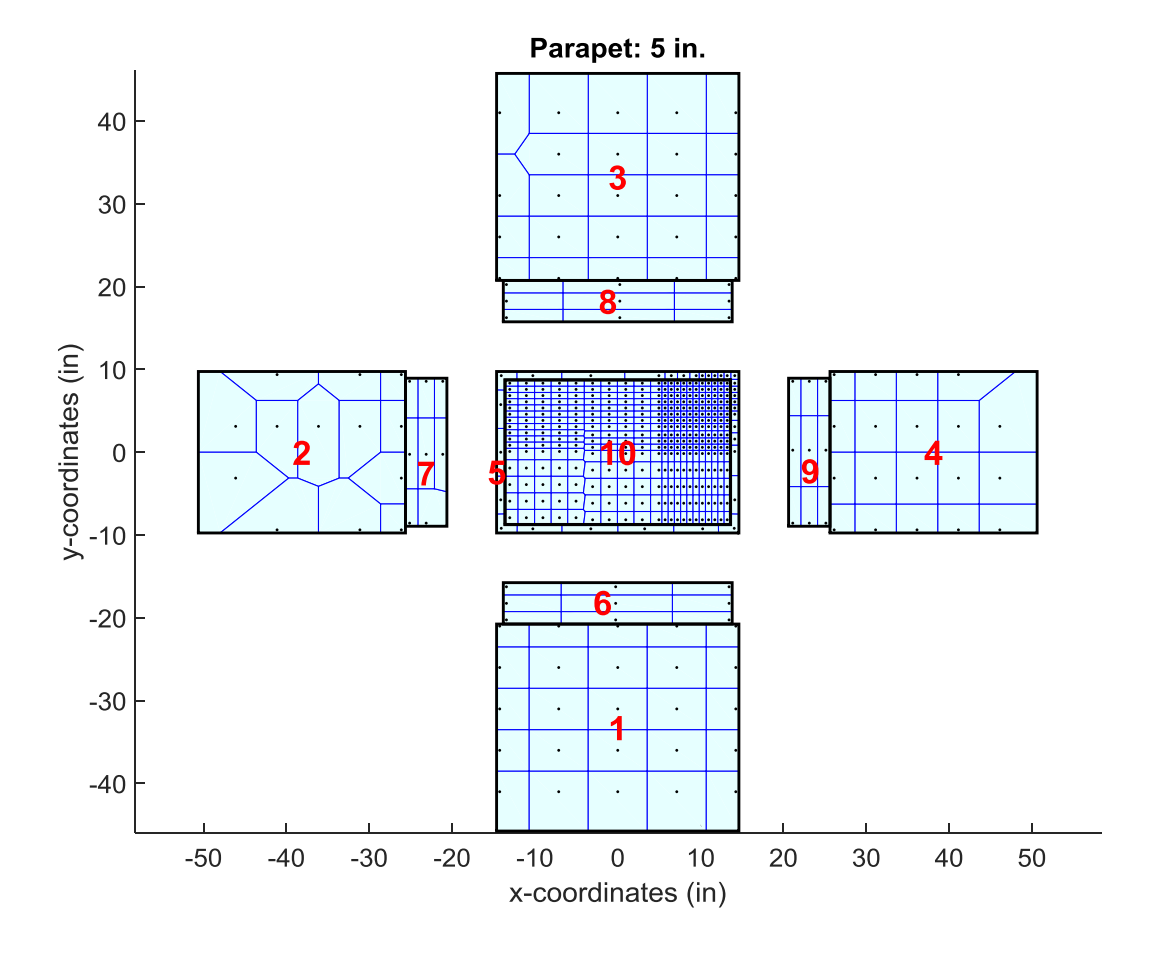


Figure 7. Tap locations and tributary areas on a flattened representation of the model with a parapet of 5 inches

5.3 Wind simulation

Simulation of upwind terrain roughness is performed via the Terraformer, an automated roughness element grid that rapidly reconfigures the height and orientation of 1116 roughness elements in a 62×18 grid to achieve desired upwind terrain conditions. The grid has a fetch length of 18.3 m. Dimensions of the elements are 5 cm by 10 cm, and they are spaced 30 cm apart in a staggered pattern. Height and orientation can be varied from 0-160 mm and 0-360 degrees, respectively. For this study, the Terraformer was configured to simulate open terrain for the given geometric scale (1:18).

Prior to placing the model in the tunnel, flow measurements were taken at the center of the test section using an automated gantry system instrumented with four Turbulent Flow Instrumentation Cobra pressure probes that measure u, v, and w velocity components and static pressure. For this study, roughness elements were raised to 20 mm and oriented with the wide edge perpendicular to the flow. Figure 8 includes the mean velocity profile and the measured longitudinal turbulence spectra at a height of 610 mm. The measured spectra was compared with the power spectra model in ESDU [13], and first derived by von Kármán for isotropic turbulence [14]. The mean velocity profile was normalized by the reference mean wind velocity U_{ref} measured at a height $z_{\text{ref}} = 1.48$ m. A roughness length estimate of 1.59 mm was obtained from a nonlinear least-squares fit of the log law in the inertial-sublayer (ISL) region ($z \sim 150-900$ mm), fol-



lowing the curve-fitting method in Karimpour et al. [15]. This results in an equivalent full-scale roughness length of 0.029 m, which is within the range of open terrain as defined in ASCE 7-10.

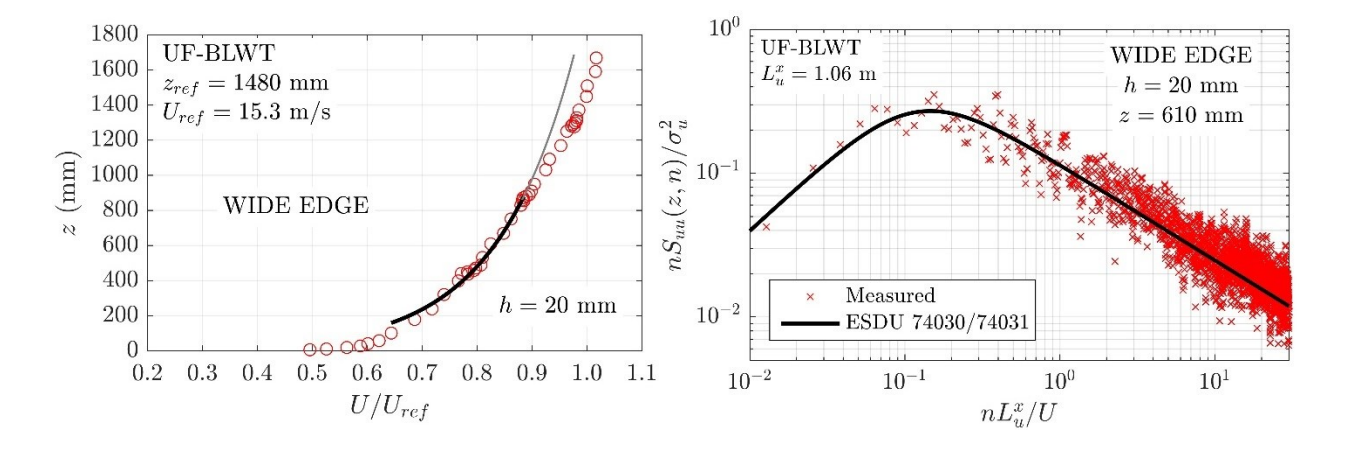


Figure 8. Mean velocity profile and longitudinal turbulence spectra (z = 610 mm) measured at the center of the test section for h = 20 mm and a wide edge windward element orientation.

5.4 Pressure coefficients

Differential pressures from 512 taps were measured simultaneously and sampled at 625 Hz. Data was collected for 120 seconds, corresponding to approximately 660 seconds full-scale assuming a basic wind speed of 40 m/s. Pressure coefficients are referenced to the velocity pressure at the model eave height. This velocity pressure was obtained indirectly by applying a reduction factor to pitot tube measurements at the freestream (z = 1.48 m). Maximum and minimum pressure coefficients were estimated from each tap pressure time history using a Fisher-Tippett Type I (Gumbel) distribution. The C_p time history was truncated into 50 segments of equal length. The peak maximum and minimum pressure coefficients from each segment were then taken, and the 78^{th} percentile is then used to estimate the maximum and minimum C_p values.

6 OPTIMIZATION SETUP

The optimization problem is physically constrained by the model-scale minimum and maximum achievable parapet height of 0 and 4.5 inches, respectively. The problem-specific particle swarm optimization (PSO) parameters of w, c_1 , and c_2 were selected to be equal in magnitude so that an equal weight would be placed on the particle's inertia, trust in itself, and trust in the swarm. After initial tests, a magnitude of 0.5 was selected for all problem-specific PSO parameters. Considering the time limits on experimental resources, a balance in needed between sufficient particles to create the PSO swarm effect and sufficient iterations to see convergence. Based on an estimated two minutes per BLWT run, one minute to set up the BLWT run, and a day of testing, five particles were selected.

The objective function is selected as a minimization of the suction on the roof, inner parapet walls, and top of the parapet considering all wind angles. As the parapet height increases, the suction decreases for the roof surface and top of the parapet wall and increases for the inner parapet wall surfaces. Critical minimum C_p values are observed for the roof, inner parapet wall,

and top of parapet at approach wind angles of 45° and 90° (Figures 9 and 10). To minimize the number of BLWT runs, each candidate solution will only be evaluated at 45° and 90° with the dense roof taps upwind.

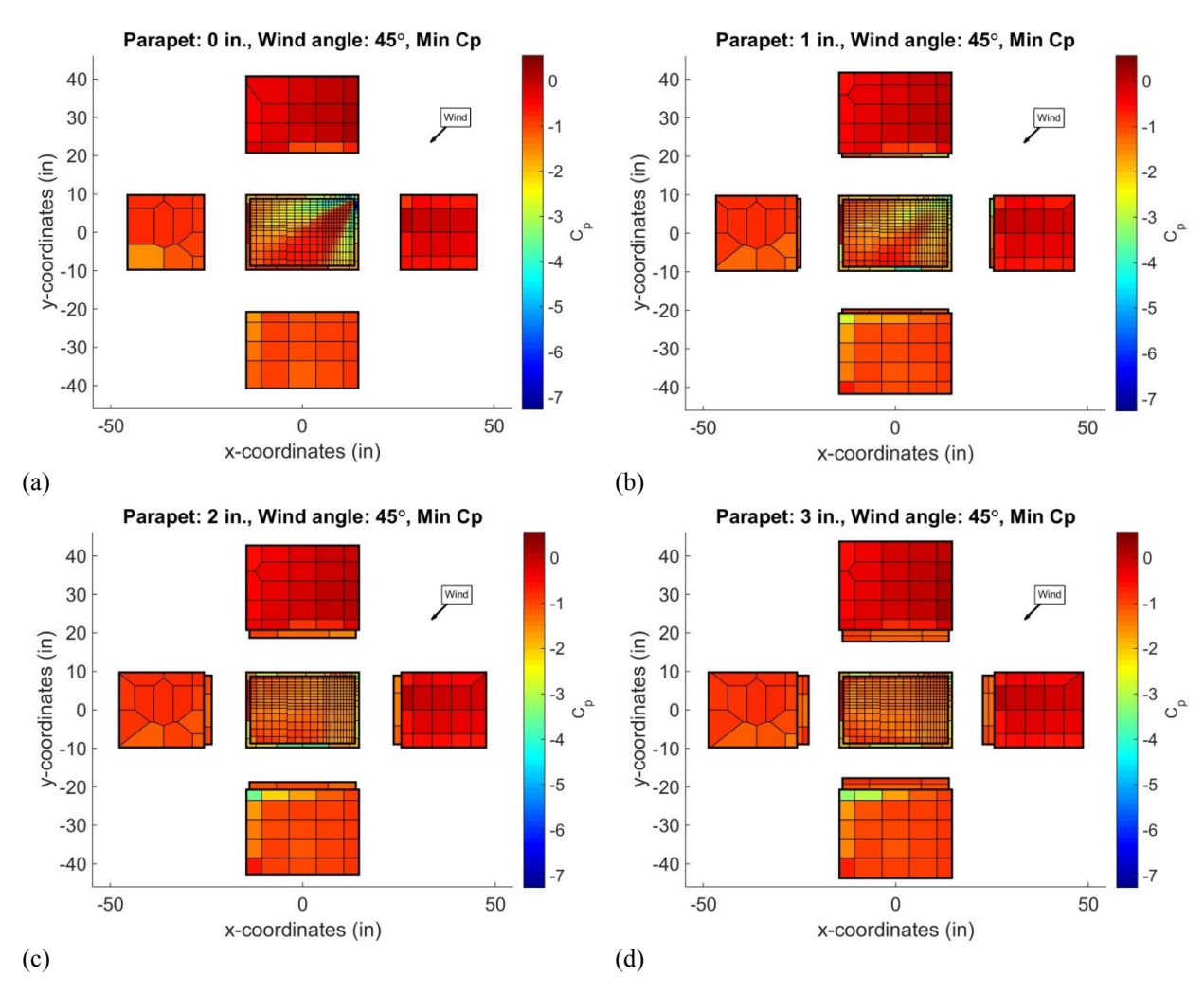


Figure 9. Minimum C_p for 45°, (a) 0 inch parapet, (b) 1 inch parapet, (c) 2 inch parapet, and (d) 3 inch parapet



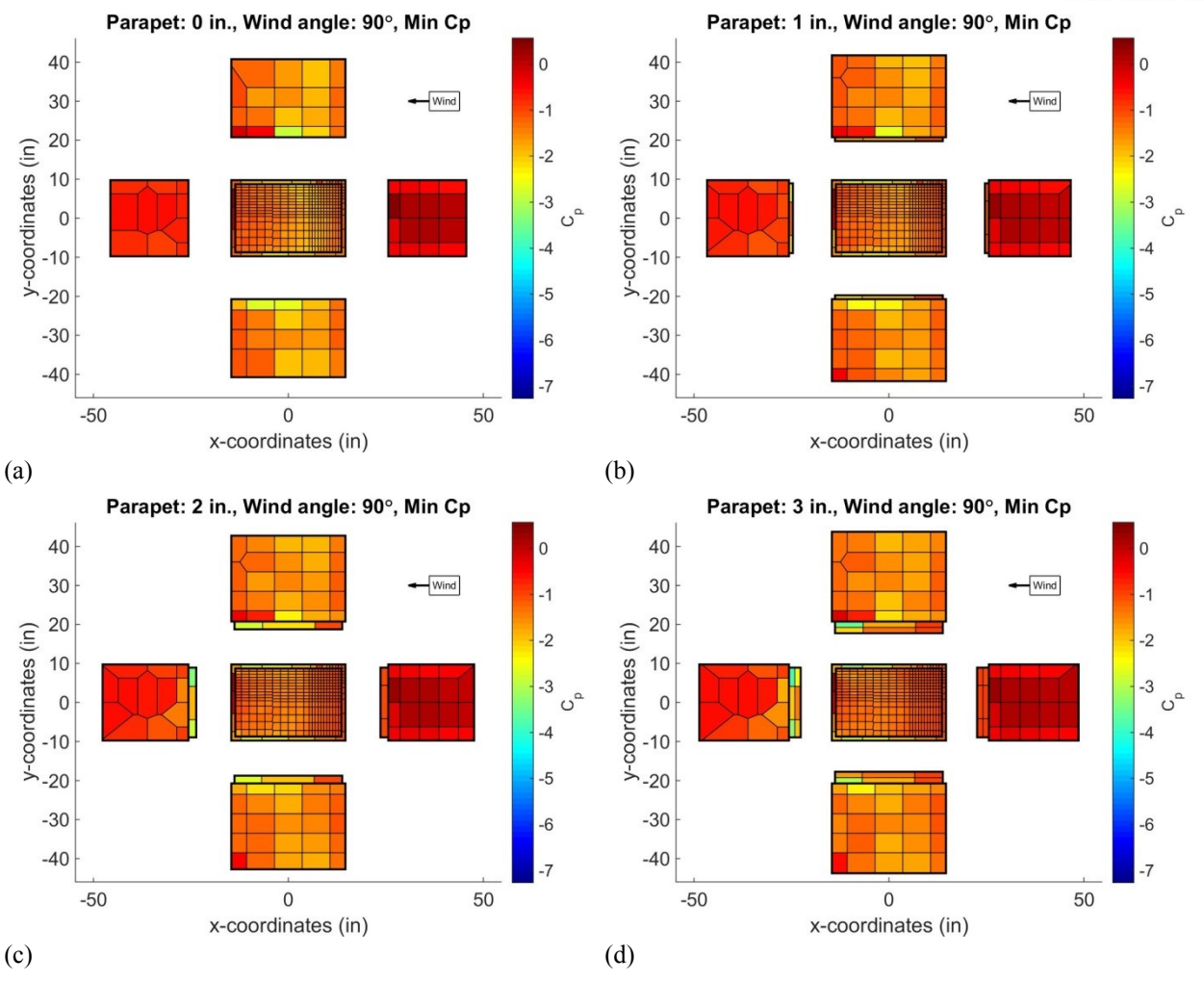


Figure 10. Minimum C_p for 90°, (a) 0 inch parapet, (b) 1 inch parapet, (c) 2 inch parapet, and (d) 3 inch parapet

7 OPTIMIZATION RESULTS AND ANALYSIS

A total of 13 design iterations were conducted for the 5 particles. The position of the particles was initially uniformly distributed across the range of positions. The convergence of the particles towards the optimum height of 2.69 inches is shown in Figure 11a. Four of the five particles converged to the global best cost. The one particle that does not converge is likely due to the particle being attracted to both its personal best cost (achieved at iteration 1) and the global best cost. The global best cost for each iteration are shown in Figure 11b. Points with both particle and cost identified represent an update to the global best cost. Figures 12 and 13 depict the envelope plot of the minimum C_p for the optimal parapet height at 45° and 90° respectively. This illustrates the balance in minimum C_p on the roof (Figure 12) and inner parapet wall surfaces (Figure 13). This balance is expected because the suction on the roof, inner parapet walls, and top of the parapet were given equal weight in the objective function.

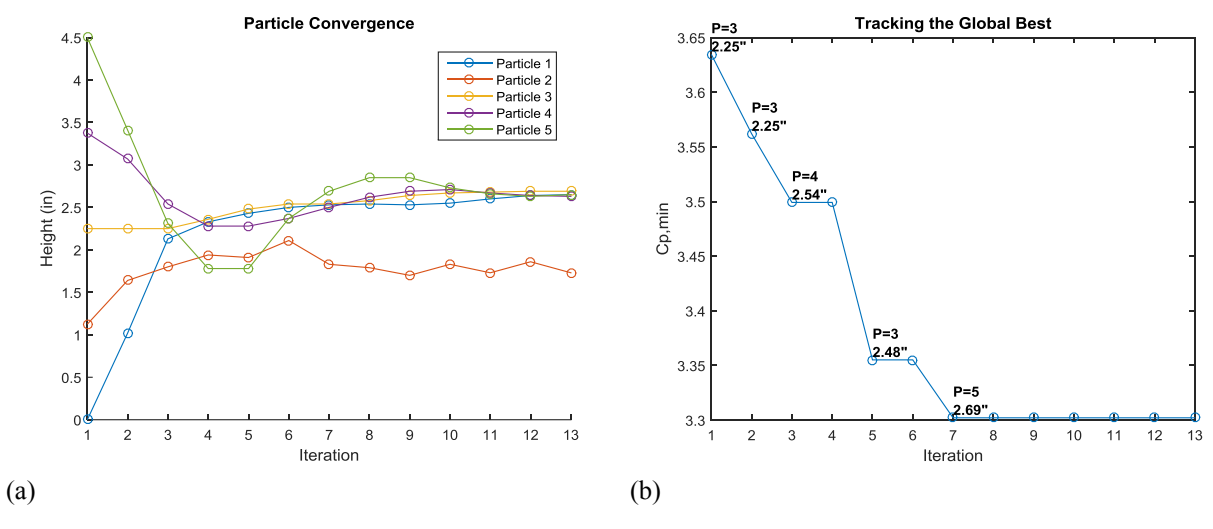


Figure 11. (a) Particle convergence at each iteration and (b) global best cost at each iteration

The optimal result corresponds to a full-scale parapet height of 4.04 feet, an otherwise non-intuitive design. This parapet height simultaneously minimizes suction on the roof and inner parapet walls. According to the Building Code Requirements for Masonry Structures, the height of structural parapets should not exceed 3 times their thickness [12]. The optimal height found satisfies this limit of 4.5 feet as applied to the current building.

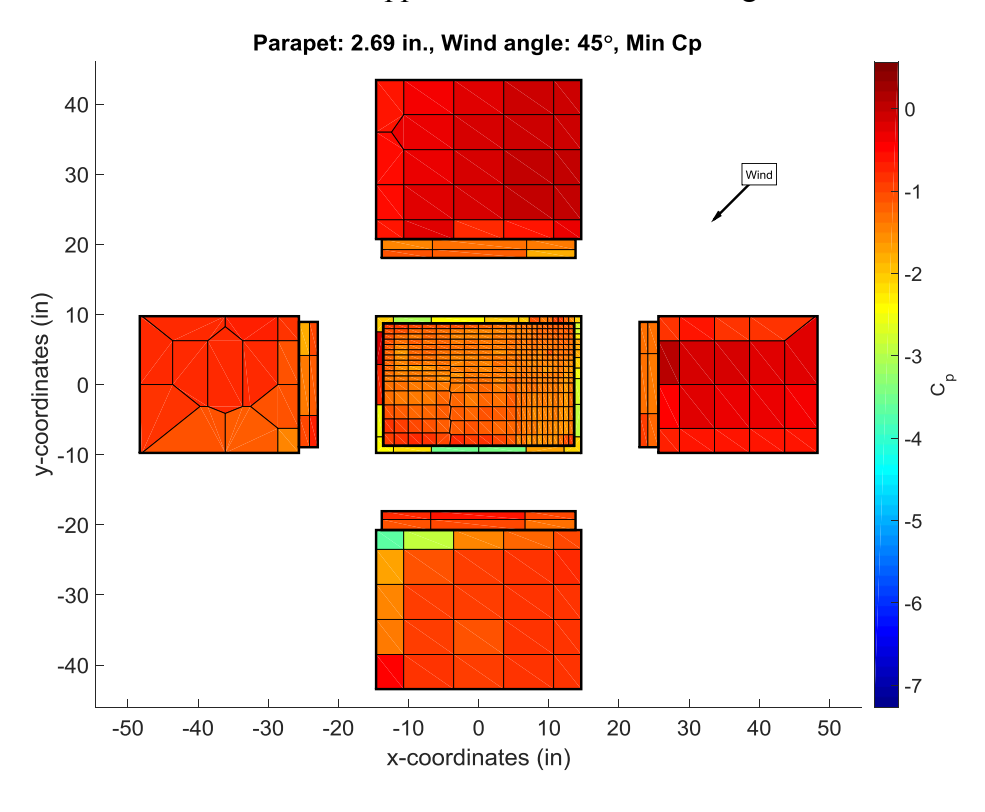


Figure 12. Minimum C_p for optimal parapet height, 45° wind angle shown



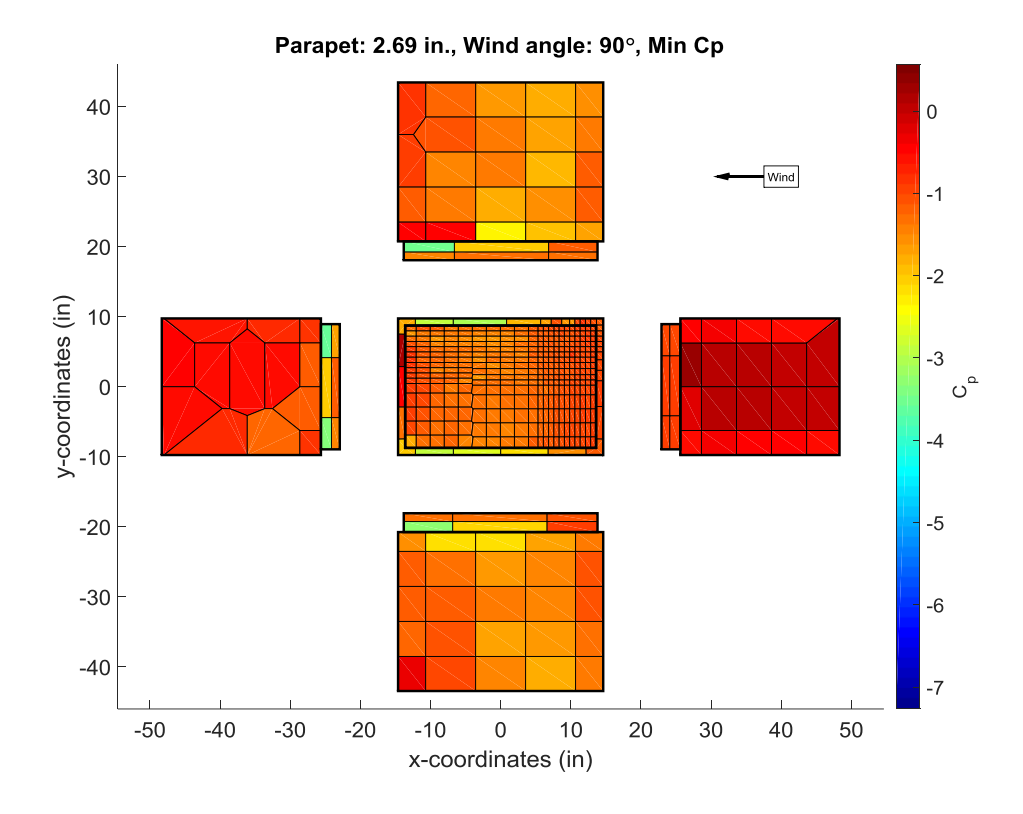


Figure 13. Minimum C_p for optimal parapet height, 90° wind angle shown

8 CONCLUSIONS

This study investigates the effect of wind on low-rise buildings with a solid parapet of variable height. The main goal is to develop a proof-of-concept cyber-physical approach to the optimal design of wind-sensitive structures. Particle swarm optimization (PSO) was used to explore the design space, producing of candidate solutions for evaluation in the BLWT. Particle swarm optimization algorithms are not problem specific, do not require gradients, and handle multiple design variables and constraints. In combination with BLWT, an accurate assessment of candidate solutions was achieved. The PSO-based approach was successful guiding the physical structure to an optimal state. Based on the objective function and constraints chosen, an optimal parapet height of 2.69 inches model-scale and 4.04 feet full-scale was found for the low-rise structure studied. Implications are significant for more complex structures where the optimal solution may not be obvious and cannot be reasonably determined with traditional experimental or computational methods.

9 ACKNOWLEDGEMENTS

This material is based upon work supported by the National Science Foundation (NSF) under Grant No. 1636039. Any opinions, findings, and conclusions or recommendations expressed in this material are those of the authors and do not necessarily reflect the views of NSF. The authors also acknowledge the NSF NHERI awardee that contributed to the research results reported

within this paper under Grant No. 1520843: Natural Hazards Engineering Research Infrastructure: Experimental Facility with Boundary Layer Wind Tunnel, Wind Load and Dynamic Flow Simulators, and Pressure Loading Actuators (University of Florida).

10 REFERENCES

- 1 ASCE, *Minimum Design Loads for Buildings and Other Structures*. (2010). Reston, VA: American Society of Civil Engineers.
- Kopp, Gregory A., et al. "Wind effects of parapets on low buildings: Part 1. Basic aerodynamics and local loads." *Journal of Wind Engineering and Industrial Aerodynamics*, vol. 93, no. 11, 10 Oct. 2005, pp. 817–841.
- Kopp, Gregory A., et al. "Wind effects of parapets on low buildings: Part 2. Structural loads." *Journal of Wind Engineering and Industrial Aerodynamics*, vol. 93, no. 11, 10 Oct. 2005, pp. 843–855.
- Kopp, Gregory A., et al. "Wind effects of parapets on low buildings: Part 3. Parapet loads." *Journal of Wind Engineering and Industrial Aerodynamics*, vol. 93, no. 11, 10 Oct. 2005, pp. 857–872.
- Kopp, Gregory A., et al. "Wind effects of parapets on low buildings: Part 4. Mitigation of corner loads with alternative geometries." *Journal of Wind Engineering and Industrial Aerodynamics*, vol. 93, no. 11, 10 Oct. 2005, pp. 873–888.
- Talbi, El-Ghazali. *Metaheuristics: From Design to Implementation*. Hoboken (NJ): John Wiley & Sons, 2009. Print.
- Perez, R. E., & Behdinan, K. (2007). Particle Swarm Optimization in Structural Design. *Swarm Intelligence: Focus on Ant and Particle Swarm Optimization*, 373-377.
- 8 He, S., et al. "An improved particle swarm optimizer for mechanical design optimization problems." *Engineering Optimization*, vol. 36, no. 5, 2004, pp. 585–605.
- 9 Stathopoulos, T., et al. "Wind loads on parapets." *Journal of Wind Engineering and Industrial Aerodynamics*, vol. 90, no. 4-5, 2002, pp. 503–514.
- Kind, R. J. "Worst suctions near edges of flat rooftops with parapets." *Journal of Wind Engineering and Industrial Aerodynamics*, vol. 31, no. 2-3, Dec. 1988, pp. 251–264.
- Pindado, S., and J. Meseguer. "Wind tunnel study on the influence of different parapets on the roof pressure distribution of low-Rise buildings." *Journal of Wind Engineering and Industrial Aerodynamics*, vol. 91, no. 9, 2003, pp. 1133–1139.
- 12 ACI/ASCE/TMS, Building code requirements and specification for masonry structures: containing Building code requirements for masonry structures (TMS 402-11/ACI 530-11 / ASCE 5-11), Specification for mason structures (TMS 602-11 / ACI 530.1-11 / ASCE 6-11) and companion commentaries / developed by the Masonry Standards Joint Committee (MSJC). Boulder, Co., The Masonry Society, 2011.
- ESDU. (1974). Characteristics of atmospheric turbulence near the ground. Part I: definitions and general information, *Engineering Sciences Data Unit*, Itm. No. 74030, 74031, London, UK.
- Karimpour, A., Kaye, N. B., and Baratian-Ghorghi, Z. (2012). "Modeling the neutrally stable atmospheric boundary layer for laboratory scale studies of the built environment." *Building and Environment*, 49, 203-211
- Von Karman, T. (1948). "Progress in the statistical theory of turbulence." *Proceedings of the National Academy of Sciences*, 34(11), 530-539.